Available online at http://ijim.srbiau.ac.ir/
Int. J. Industrial Mathematics (ISSN 2008-5621)
Vol. 7, No. 1, 2015 Article ID IJIM-00583, 11 pages
Research Article

The effects of MHD flow of third grade fluid by means of meshless local radial point interpolation (MLRPI)

S. Abbasbandy *†, E. Shivanian ‡

Abstract

The meshless local radial point interpolation (MLRPI) method is applied to examine the magneto-hydrodynamic (MHD) flow of third grade fluid in a porous medium. The fluid saturates the porous space between the two boundaries. Several limiting cases of fundamental flows can be obtained as the special cases of present analysis. The variations of pertinent parameters are addressed.

Keywords : Porous medium; Magnetohydrodynamic; Non-Newtonian fluid; Local weak formulation; Meshless local radial point interpolation.

1 Introduction

The flow inside porous space encounters in several systems, ranging from natural to Man-manufactured technological ones. Examples of porous space include rye bread, lime stone, oil wells, chemical catalysts, underground aquifers, wood etc. The flows of non-Newtonian fluids [1, 2, 3, 4]) are also significant in many engineering applications. Recently, the flows of one-dimensional second grade [5]) and Oldroyd-B [6]) fluids are discussed. Mathematical formulation in these articles has been presented employing the modified Darcy's law and the mathematical problems were linear. However, the one-dimensional flow of third grade fluid even in steady situation constructs nonlinear differential equation. This equation for flow in porous space through Modified Darcy's law is more nonlinear. Also, the consideration of grade fluid predicts the shear thinning/shear thickening effects even in steady flows. Thus, the objective of present article is to consider some fundamental flows of third grade fluid in a porous space. The magnetohydrodynamic (MHD) fluid fills the porous space between the two boundaries. The fluid is electrically conducting in the presence of applied magnetic field. Constant pressure gradient is also considered. Hence we investigate the more general differential system in usual notation satisfying

$$\frac{d^2u}{dy^2} + 2\beta\frac{d}{dy}\left(\frac{du}{dy}\right)^3 - \frac{1}{K}\left[1 + 2\beta\left(\frac{du}{dy}\right)^2\right]u - Mu = C, \quad (1.1)$$

$$u(a) = c \qquad u(b) = d, \quad (1.2)$$

where β, M, K, C are the third grade parameter, permeability parameter, magnetic parameter and pressure gradient parameter. Here u is the velocity in the x-direction.

The main shortcoming of mesh-based methods such as the finite element method (FEM),

*Corresponding author. abbasbandy@yahoo.com
†Department of Mathematics, Imam Khomeini International University, Ghazvin, 34149-16818, Iran.
‡Department of Mathematics, Imam Khomeini International University, Ghazvin, 34149-16818, Iran.

the finite volume method (FVM) and the boundary element method (BEM) is that these numerical methods rely on meshes or elements. In the last two decades, in order to overcome the mentioned difficulties some techniques the so-called meshless methods have been proposed [7]. This method is used to establish system of algebraic equations for the whole domain of the problem without the use of predefined mesh for the domain discretization so that set of nodes scattered within the domain of the problem as well as sets of nodes on the boundaries of the domain to represent (but not to discretize) the domain of the problem and its boundaries is used. These sets of scattered nodes are usually called field nodes. There are three types of meshless methods: meshless methods based on weak forms such as the element free Galerkin (EFG) method [8, 9], meshless methods based on collocation techniques (strong forms) such as the meshless collocation method based on radial basis functions (RBFs) [10, 11] and meshless methods based on the combination of weak forms and collocation technique. Due to the ill-conditioning of the resultant linear systems in RBF-collocation method, various approaches are proposed to circumvent this problem, Refs. [12, 13, 14, 15] being among them. The weak forms are used to derive a set of algebraic equations through a numerical integration process using a set of quadrature domain that may be constructed globally or locally in the domain of the problem. In the global weak form methods, global background cells are needed for numerical integration in computing the algebraic equations. To avoid the use of global background cells, a so-called local weak form is used to develop the meshless local Petrov-Galerkin (MLPG) method [16, 17, 18, 19, 20, 21, 23]. When a local weak form is used for a field node, the numerical integrations are carried out over a local quadrature domain defined for the node, which can also be the local domain where the test (weight) function is defined. The local domain usually has a regular and simple shape for an internal node (such as sphere, rectangular, etc.), and the integration is done numerically within the local domain. Hence the domain and boundary integrals in the weak form methods can easily be evaluated over the regularly shaped subdomains(spheres in 3D or circles in 2D) and their boundaries. In the literature, several meshless weak form methods have been reported such as diffuse element method (DEM) [24], smooth particle hydrodynamic (SPH) [25, 26], the reproducing kernel particle method (RKPM) [27], boundary node method (BNM) [28], partition of unity finite element method (PUFEM) [29], finite sphere method (FSM) [30], boundary point interpolation method (BPIM) [31] and boundary radial point interpolation method (BRPIM) [32]. Liu applied the concept of MLPG and developed meshless local radial point interpolation (MLRPI) method [33, 34, 35]. In this paper, the problem (1.1)-(1.2) will be solved by meshless local radial point interpolation (MLRPI) method [36]. It is noticed that for plane Couette flow we have $C = c = 0$; Plug flow corresponds to $C = 0$; Poiseuille flow when $c = d = 0$ and generalized Couette flow when $c = 0$. Graphical results for different parameters are given and examined.

2 The modified radial point interpolation scheme

In the conventional point interpolation method (PIM) there is a main difficulty that inverse of the polynomial moment matrix (it will be defined later) does not often exist. This condition could always be possible depending on the locations of the nodes in the support domain and the terms of monomials used in the basis. If an inappropriate polynomial basis is chosen for a given set of nodes, it may yield in a badly conditioned or even singular moment matrix [7]. In order to avoid the singularity problem in the polynomial point interpolation method (PIM), the radial basis function (RBF)is used to develop the radial point interpolation method (RPIM) for meshless weak form techniques [34, 37, 38]. The combination of RPIM and polynomial PIM is described as follows: consider a continuous function $u(x)$ defined in a domain Ω, which is represented by a set of field nodes. The $u(x)$ at a point of interest x is approximated in the form of

$$u(\mathbf{x}) = \sum_{i=1}^{n} R_i(\mathbf{x})\, a_i + \sum_{j=1}^{m} p_j(\mathbf{x})\, b_j = \mathbf{R}^T(\mathbf{x})\, \mathbf{a} + \mathbf{P}^T(\mathbf{x})\, \mathbf{b}\,, \quad (2.3)$$

where $R_i(\mathbf{x})$ is a radial basis function (RBF), n is the number of RBFs, $p_j(\mathbf{x})$ is monomial in the

space coordinate x and m is the number of polynomial basis functions. The $p_j(x)$ in Eq. (2.3) is, in general, chosen in a top-down approach from the Pascal triangle, so that the basis is complete to a desired order and a complete basis is usually preferred. For 1-D problems, we use

$$\mathbf{P}^T(\mathbf{x}) \;=\; \{\, 1, x, x^2, x^3, ..., x^m \,\}\;, \qquad (2.4)$$

For 2-D problems, we shall have

$$\begin{aligned}\mathbf{P}^T(\mathbf{x}) &= \mathbf{P}^T(x,y)\\ &= \{1, x, y, xy, x^2, y^2, \ldots, x^m, y^m\}\,, \end{aligned} \qquad (2.5)$$

and etc. When $m = 0$, only RBFs are used, otherwise the RBF is augmented with m polynomial basis functions. Coefficients a_i and b_j are unknown which should be determined. There are some types of RBFs, and the characteristics of RBFs have been widely investigated [10, 39, 40]. In the current work, we have chosen the thin plate spline (TPS) as radial basis functions in Eq. (2.3). This RBF is defined as follows:

$$R(\mathbf{x}) \;=\; r^{2m}\,\ln(r)\,, \qquad m \;=\; 1\,,\,2\,,\,3\,,\,\ldots\,. \qquad (2.6)$$

Since $R(\mathbf{x})$ in Eq. (2.6) belongs to C^{2m-1} (all continuous function to the order $2m-1$), so higher-order thin plate splines must be used for higher-order partial differential operators. For the second-order partial differential equation (1.1), $m = 2$ is used for thin plate splines (i.e., second-order thin plate splines). In the radial basis function $R_i(\mathbf{x})$, the variable is only the distance between the point of interest x and a node at x_i, i.e., $r = |\, x - x_i \,|$ for 1-D and $r = \sqrt{(x-x_i)^2 + (y-y_i)^2}$ for 2-D. In order to determine a_i and b_j in Eq. (2.3), a support domain is formed for the point of interest at x, and n field nodes are included in the support domain. Coefficients a_i and b_j in Eq. (2.3) can be determined by enforcing Eq. (2.3) to be satisfied at these n nodes surrounding the point of interest x. This leads to the system of n linear equations, one for each node. The matrix form of these equations can be expressed as

$$\mathbf{U}_s \;=\; \mathbf{R}_n\,\mathbf{a} \;+\; \mathbf{P}_m\,\mathbf{b}\,, \qquad (2.7)$$

where the vector of function values U_s is

$$\mathbf{U}_s \;=\; \{\, u_1\,,\; u_2\,,\; u_3\,,\; \ldots\,,\; u_n\,\}^T\;, \qquad (2.8)$$

the RBFs moment matrix is

$$\mathbf{R}_n = \begin{bmatrix} R_1(r_1) & R_2(r_1) & ... & R_n(r_1) \\ R_1(r_2) & R_2(r_2) & ... & R_n(r_2) \\ \vdots & \vdots & \ddots & \vdots \\ R_1(r_n) & R_2(r_n) & ... & R_n(r_n) \end{bmatrix}_{n\times n}\;, \qquad (2.9)$$

and the polynomial moment matrix is

$$\mathbf{P}_m \;=\; \begin{bmatrix} 1 & x_1 & ... & x_1^m \\ 1 & x_2 & ... & x_2^m \\ \vdots & \vdots & \ddots & \vdots \\ 1 & x_n & ... & x_n^m \end{bmatrix}_{n\times m}\;. \qquad (2.10)$$

Also, the vector of unknown coefficients for RBFs is

$$\mathbf{a}^T \;=\; \{\, a_1\,,\; a_2\,,\; a_3\,,\; \ldots\,,\; a_n\,\}\;, \qquad (2.11)$$

and the vector of unknown coefficients for polynomial is

$$\mathbf{b}^T \;=\; \{\, b_1\,,\; b_2\,,\; b_3\,,\; \ldots\,,\; b_m\,\}\;. \qquad (2.12)$$

We notify that, in Eq. (2.9), r_k in $R_i(r_k)$ is defined as

$$r_k \;=|\, x_k \;-\; x_i \,|\;\;. \qquad (2.13)$$

We mention that there are $m+n$ variables in Eq. (2.7). The additional m equations can be added using the following m constraint conditions:

$$\sum_{i\,=\,1}^{n} p_j(\mathbf{x}_i)\,a_i \;=\; \mathbf{P}_m^T\mathbf{a} \;=\; 0\,, \qquad ,j \;=\; 1\,,2\,,\ldots,\;m\,. \qquad (2.14)$$

Combining Eqs. (2.7) and (2.14) yields the following system of equations in the matrix form:

$$\tilde{\mathbf{U}}_s \;=\; \begin{bmatrix} \mathbf{U}_s \\ 0 \end{bmatrix} \;=\; \begin{bmatrix} \mathbf{R}_n & \mathbf{P}_m \\ \mathbf{P}_m^T & 0 \end{bmatrix} \begin{bmatrix} \mathbf{a} \\ \mathbf{b} \end{bmatrix} \;=\; \mathbf{G}\,\tilde{\mathbf{a}}\,, \qquad (2.15)$$

where

$$\begin{aligned}\tilde{\mathbf{U}}_s \;&=\; \{\, u_1\,u_2\,\ldots\,u_n\,0\,0\,\ldots\,0\,\}\;,\\ \tilde{\mathbf{a}}^T \;&=\; \{\, a_1\,a_2\,\ldots\,a_n\,b_1\,\ldots\,b_m\,\}\;. \end{aligned} \qquad (2.16)$$

Because the matrix R_n is symmetric, the matrix G will also be symmetric. Solving Eq. (2.15), we obtain

$$\tilde{\mathbf{a}} \;=\; \begin{bmatrix} \mathbf{a} \\ \mathbf{b} \end{bmatrix} \;=\; \mathbf{G}^{-1}\,\tilde{\mathbf{U}}_s\,. \qquad (2.17)$$

Eq. (2.3) can be rewritten as

$$\begin{aligned} u(\mathbf{x}) \;&=\; \mathbf{R}^T(\mathbf{x})\,\mathbf{a} \;+\; \mathbf{P}^T(\mathbf{x})\,\mathbf{b}\\ &=\; \{\, \mathbf{R}^T(\mathbf{x})\,,\, \mathbf{P}^T(\mathbf{x})\,\} \begin{bmatrix} \mathbf{a} \\ \mathbf{b} \end{bmatrix}. \end{aligned} \qquad (2.18)$$

Now using Eq. (2.17), we obtain

$$u(\mathbf{x}) = \{ \mathbf{R}^T(\mathbf{x}) , \mathbf{P}^T(\mathbf{x}) \} \mathbf{G}^{-1} \tilde{\mathbf{U}}_s = \tilde{\Phi}^T(\mathbf{x}) \tilde{\mathbf{U}}_s , \quad (2.19)$$

where $\tilde{\Phi}^T(\mathbf{x})$ can be rewritten as

$$\begin{aligned} \tilde{\Phi}^T(\mathbf{x}) &= \{ \mathbf{R}^T(\mathbf{x}) , \mathbf{P}^T(\mathbf{x}) \} \mathbf{G}^{-1} \\ &= \{ \phi_1(\mathbf{x}) \, \phi_2(\mathbf{x}) \, ... \, \phi_n(\mathbf{x}) \, \phi_{n+1}(\mathbf{x}) \\ &\quad ... \, \phi_{n+m}(\mathbf{x}) \} . \end{aligned} \quad (2.20)$$

The first n functions of the above vector function are called the RPIM shape functions corresponding to the nodal displacements. We show by the vector $\tilde{\Phi}^T(\mathbf{x})$ so that it is

$$\tilde{\Phi}^T(\mathbf{x}) = \{ \phi_1(\mathbf{x}) \, \phi_2(\mathbf{x}) \, ... \, \phi_n(\mathbf{x}) \} , \quad (2.21)$$

then Eq. (2.19) is converted to the following one:

$$u(\mathbf{x}) = \tilde{\Phi}^T(\mathbf{x}) \mathbf{U}_s = \sum_{i=1}^{n} \phi_i(\mathbf{x}) \, u_i . \quad (2.22)$$

The derivatives of $u(\mathbf{x})$ are easily obtained as

$$\begin{aligned} \frac{\partial u(\mathbf{x})}{\partial x} &= \sum_{i=1}^{n} \frac{\partial \phi_i(\mathbf{x})}{\partial x} u_i , \\ \frac{\partial^2 u(\mathbf{x})}{\partial x^2} &= \sum_{i=1}^{n} \frac{\partial^2 \phi_i(\mathbf{x})}{\partial x^2} u_i . \end{aligned} \quad (2.23)$$

Note that $\mathbf{R}_n^{-1}$ usually exists for arbitrary scattered nodes and therefore the augmented matrix G is theoretically non-singular [41, 42]. In addition, the order of polynomial used in Eq. (2.3) is relatively low. We add that the RPIM shape functions have the Kronecker delta function property, that is

$$\phi_i(\mathbf{x}_j) = \begin{cases} 1 , & i = j , \; j = 1 , 2, ... , n , \\ 0 , & i \neq j , \; j = 1 , 2, ... , n . \end{cases} \quad (2.24)$$

This is be cause the RPIM shape functions are created to pass through nodal values.

3 The meshless local weak form formulation

Instead of giving the global weak form, the ML-RPI method constructs the weak form over local quadrature cell such as Ω_q, which is a small region taken for each node in the global domain Ω. The local quadrature cells overlap with each other and cover the whole global domain Ω. The local quadrature cells could be of any geometric shape and size. In one dimensional problems, they are lines (intervals). The local weak form of Eq. (1.1) for $\mathbf{y}_i \in \Omega_q^i = (y_i - r_q, y_i + r_q)$, can be written as

$$\begin{aligned} &\int_{\Omega_q^i} \frac{d^2 u}{dy^2} \nu(\mathbf{y}) dy \\ &\quad - \left(\frac{1}{K} + M \right) \int_{\Omega_q^i} u \nu(\mathbf{y}) dy = \\ &\quad \frac{2\beta}{K} \int_{\Omega_q^i} \tilde{u} \left(\frac{d\tilde{u}}{dy} \right)^2 \nu(\mathbf{y}) dy \\ &\quad - 6\beta \int_{\Omega_q^i} \frac{d^2 \tilde{u}}{dy^2} \left(\frac{d\tilde{u}}{dy} \right)^2 \nu(\mathbf{y}) dy \\ &\quad + C \int_{\Omega_q^i} \nu(\mathbf{y}) dy, \end{aligned} \quad (3.25)$$

where Ω_q^i is the local quadrature domain associated with the point i, and $\nu(\mathbf{y})$ is the Heaviside step function

$$\nu(\mathbf{y}) = \begin{cases} 1 , & y \in \Omega_q , \\ 0 , & y \notin \Omega_q , \end{cases} \quad (3.26)$$

as the test function in each local quadrature domain. Also, $\tilde{u}$ is the latest available approximation of u to treat the nonlinearity of the problem by a simple predictor-corrector method. Using integration by parts, one has

$$\begin{aligned} &\int_{\Omega_q^i} \frac{d^2 u(\mathbf{y})}{d\mathbf{y}^2} \nu(\mathbf{y}) dx \\ &\quad = \nu(\mathbf{y}) \frac{du(\mathbf{y})}{d\mathbf{y}} \Big|_{\mathbf{y}=y_i-r_q}^{\mathbf{y}=y_i+r_q} \\ &\quad - \int_{\Omega_q^i} \frac{du(\mathbf{y})}{d\mathbf{y}} \frac{d\nu(\mathbf{y})}{dy} dy \\ &\quad = \frac{du(\mathbf{y})}{d\mathbf{y}} \Big|_{\mathbf{y}=y_i-r_q}^{\mathbf{y}=y_i+r_q}, \end{aligned} \quad (3.27)$$

and using the test function the following local weak equation will be obtained

$$\begin{aligned} &\frac{du(\mathbf{y})}{d\mathbf{y}} \Big|_{\mathbf{y}=y_i-r_q}^{\mathbf{y}=y_i+r_q} - \left(\frac{1}{K} + M \right) \int_{\Omega_q^i} u dy = \\ &\frac{4 r_q \beta}{K} \tilde{u} \left(\frac{d\tilde{u}}{dy} \right)^2 - 12 r_q \beta \frac{d^2 \tilde{u}}{dy^2} \left(\frac{d\tilde{u}}{dy} \right)^2 + 2 r_q C. \end{aligned} \quad (3.28)$$

Applying the radial point interpolation method (RPIM) for the unknown functions, the local integral equation (4.29) is transformed in to a system of algebraic equations with used unknown quantities, as described in the next section.

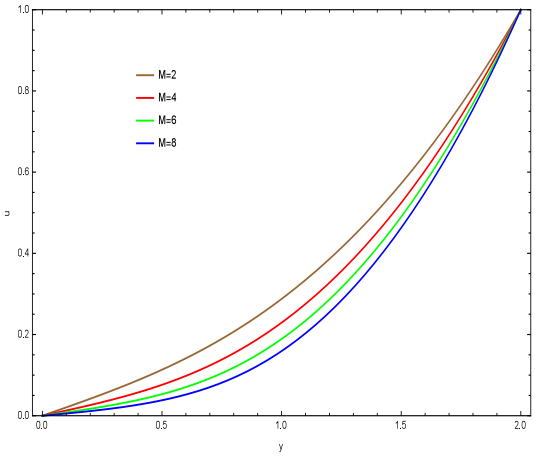

Figure 1: Variation of M on u when $K = 1$ and $\beta = 1$.

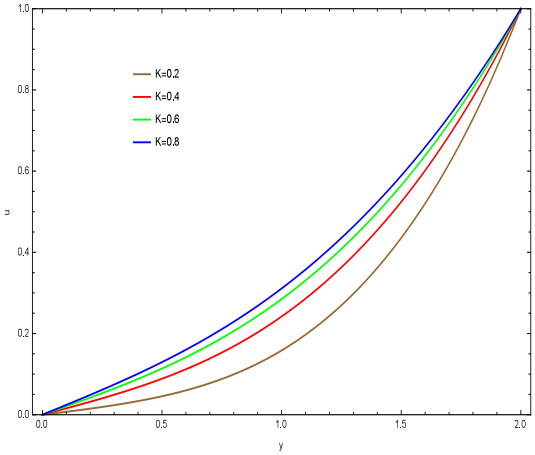

Figure 2: Variation of K on u when $M = 1$ and $\beta = 1$.

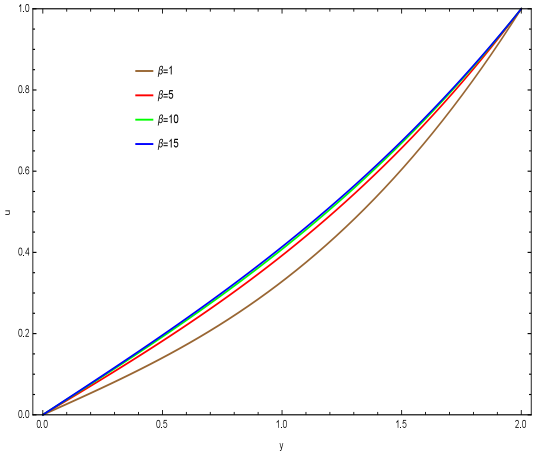

Figure 3: Variation of β on u when $M = 1$ and $K = 1$.

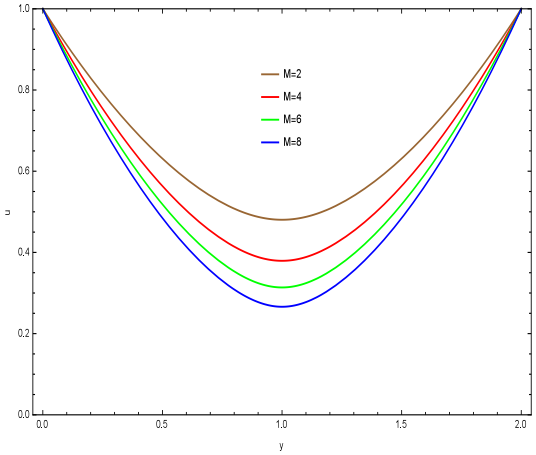

Figure 4: Variation of M on u when $K = 1$ and $\beta = 1$.

4 Discretization for MLRPI method

In this section, we consider Eq. (4.29) to see how to obtain discrete equations and apply a simple predictor-corrector procedure to overcome the nonlinearity of the problem. Consider N regularly located points on the boundary and domain of the problem so that the distance between two consecutive nodes is constant and equal to h. Assuming that $u^{(k)}(\mathbf{y}_i), i = 1, 2, ..., N$ are known, our aim is to compute $u^{(k+1)}(\mathbf{y}_i), i = 1, 2, ..., N$. So, we have N unknowns and to compute these unknowns, we need N equations. As it will be described, corresponding to each node we obtain one equation.

For nodes which are located in the interior of the domain, i.e., for $\mathbf{y}_i \in$ interior Ω, to obtain the discrete equations from the locally weak forms (4.29), substituting approximation formulas (2.22) and (2.23) in to local integral equations

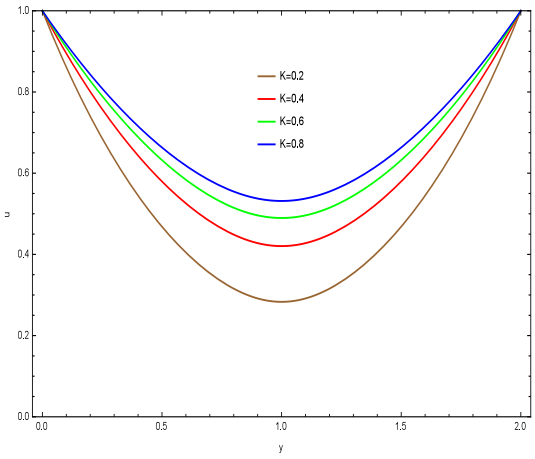

Figure 5: Variation of K on u when $M = 1$ and $\beta = 1$.

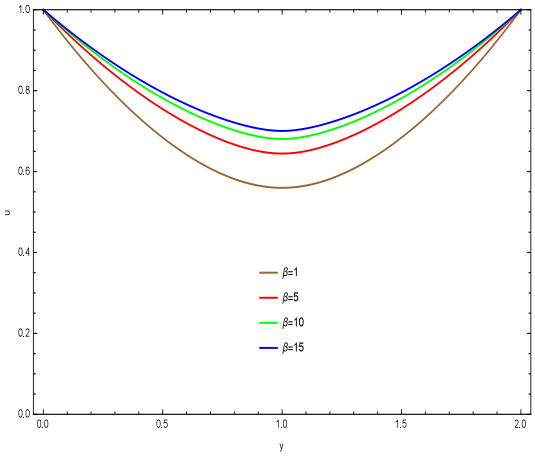

Figure 6: Variation of β on u when $M = 1$ and $K = 1$.

(4.29) yields

$$\sum_{j=1}^{N} u_j^{(k+1)} \frac{d\phi_j(\mathbf{y})}{d\mathbf{y}}\Big|_{\mathbf{y}=y_i-r_q}^{\mathbf{y}=y_i+r_q} - (\frac{1}{K}+M)\sum_{j=1}^{N}(\int_{\Omega_q^i}\phi_j(\mathbf{y})dy)u_j^{(k+1)} = [\frac{4r_q\beta}{K}(\sum_{j=1}^{N}\phi_j(\mathbf{y})u_j^{(k)})(\sum_{j=1}^{N}\frac{d\phi_j(\mathbf{y})}{d\mathbf{y}}u_j^{(k)})^2]_{\mathbf{y}=y_i} - [12r_q\beta(\sum_{j=1}^{N}\frac{d^2\phi_j(\mathbf{y})}{d\mathbf{y}^2}u_j^{(k)})(\sum_{j=1}^{N}\frac{d\phi_j(\mathbf{y})}{d\mathbf{y}}u_j^{(k)})^2]_{\mathbf{y}=y_i} + 2r_qC, \quad (4.29)$$

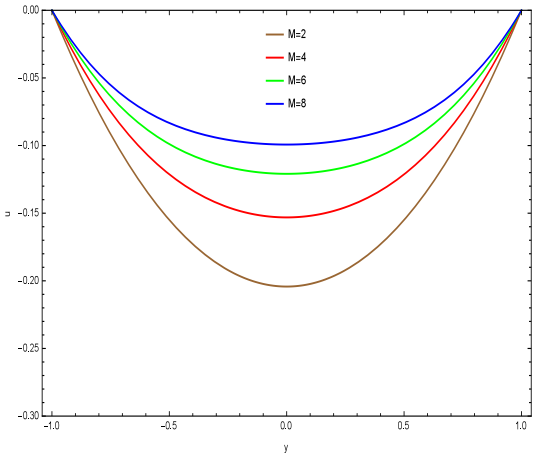

Figure 7: Effect of M on u when $C = 1$, $K = 1$ and $\beta = 1$.

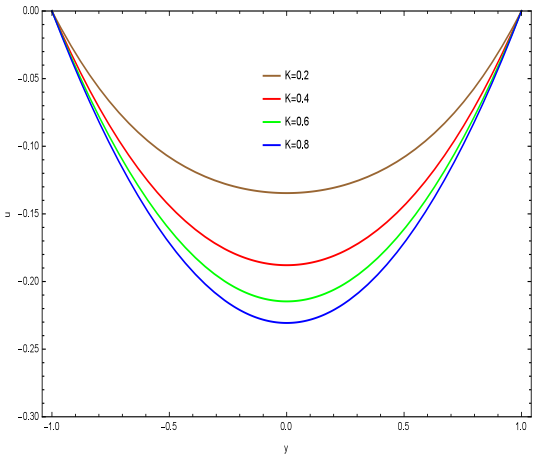

Figure 8: Effect of K on u when $C = 1$, $M = 1$ and $\beta = 1$.

or equivalently

$$\sum_{j=1}^{N}[(\frac{d\phi_j(\mathbf{y})}{d\mathbf{y}}\Big|_{\mathbf{y}=y_i+r_q} - \frac{d\phi_j(\mathbf{y})}{d\mathbf{y}}\Big|_{\mathbf{y}=y_i-r_q}) - (\frac{1}{K}+M)(\int_{y_i-r_q}^{y_i+r_q}\phi_j(\mathbf{y})dy)]u_j^{(k+1)} = [\frac{4r_q\beta}{K}(\sum_{j=1}^{N}\phi_j(\mathbf{y})u_j^{(k)})\times (\sum_{j=1}^{N}\frac{d\phi_j(\mathbf{y})}{d\mathbf{y}}u_j^{(k)})^2]_{\mathbf{y}=y_i} - [12r_q\beta(\sum_{j=1}^{N}\frac{d^2\phi_j(\mathbf{y})}{d\mathbf{y}^2}u_j^{(k)})\times (\sum_{j=1}^{N}\frac{d\phi_j(\mathbf{y})}{d\mathbf{y}}u_j^{(k)})^2]_{\mathbf{y}=y_i} + 2r_qC. \quad (4.30)$$

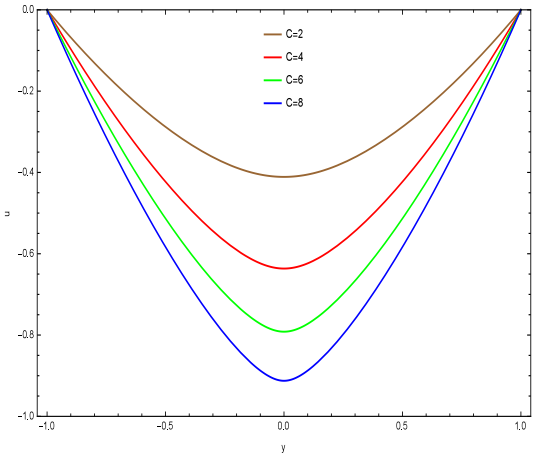

Figure 9: Effect of C on u when $\beta = 1$, $M = 1$ and $K = 1$.

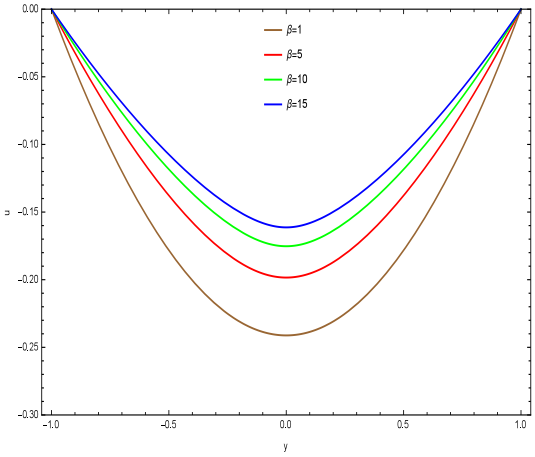

Figure 10: Effect of β on u when $C = 1$, $M = 1$ and $K = 1$.

The number of equations in the above system is $N - 2$ because we have the number of $N - 2$ interior nodes. For nodes which are located on the boundary, from (1.2), we have

$$u^{k+1}(a) = c, \qquad u^{k+1}(b) = d. \tag{4.31}$$

Therefore, Eqs. (4.30) and (4.31) provide us a linear system of N equations with N unknowns which can be solved iteratively until convergence occurs. In the next section, we have used the criteria $\|U^{(k+1)} - U^{(k)}\|_\infty \leq 10^{-10}$ to stop the procedure of solving the system iteratively.

5 Numerical experiments

In this section, we discuss the numerical results for magnetic, porosity and third grade parameters.

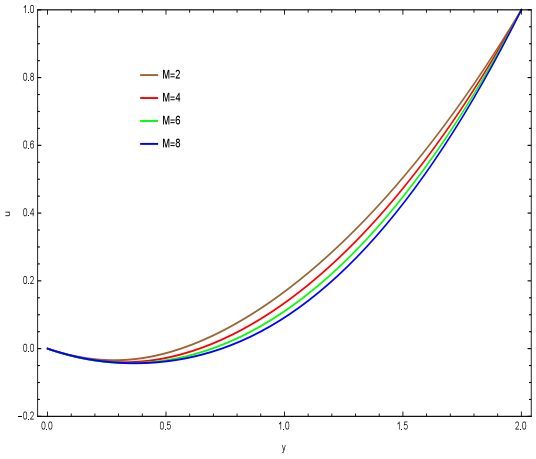

Figure 11: Effect of M on u when $C = 1$, $K = 1$ and $\beta = 1$.

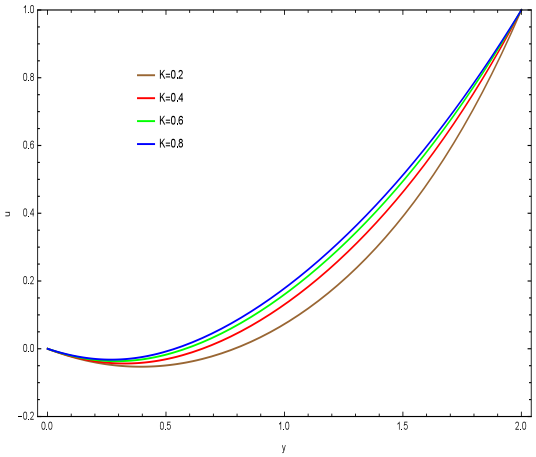

Figure 12: Effect of K on u when $C = 1$, $M = 1$ and $\beta = 1$.

5.1 Plane Couette Flow Problem

We consider the flow between two boundaries in the absence of pressure gradient. The upper boundary is suddenly moved. Here the mathematical problem is

$$\frac{d^2u}{dy^2} + 2\beta \frac{d}{dy}\left(\frac{du}{dy}\right)^3 - \frac{1}{K}\left[1 + 2\beta\left(\frac{du}{dy}\right)^2\right] u - Mu = 0, \tag{5.32}$$

with boundary conditions

$$u(0) = 0 \qquad u(2) = 1. \tag{5.33}$$

The Figs. 1 to 3 have been prepared to explain the effects of plane Couette flow between two boundaries in the absence of pressure gradient.

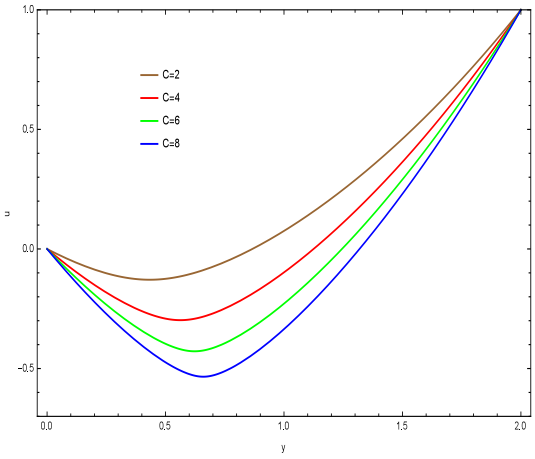

Figure 13: Effect of C on u when $\beta = 1$, $M = 1$ and $K = 1$.

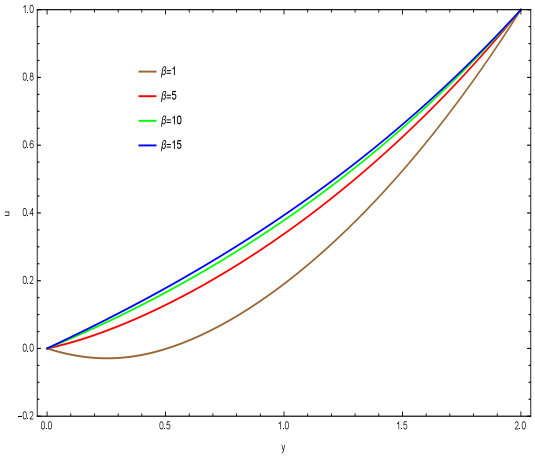

Figure 14: Effect of β on u when $C = 1$, $M = 1$ and $K = 1$.

5.2 Plug Flow Problem

Here we investigate the flow due to sudden motion of two boundaries. The mathematical equation here is

$$\frac{d^2u}{dy^2} + 2\beta\frac{d}{dy}\left(\frac{du}{dy}\right)^3 - \frac{1}{K}\left[1 + 2\beta\left(\frac{du}{dy}\right)^2\right]u - Mu = 0, \quad (5.34)$$

with boundary conditions

$$u(0) = 1 \qquad u(2) = 1. \quad (5.35)$$

Figs. 4 to 6 have been displayed for plug flow due to sudden motion of two boundaries.

5.3 Fully developed plane Poiseuille Flow Problem

This subsection deals with the flow in presence of applied pressure gradient. The problem reduces to

$$\frac{d^2u}{dy^2} + 2\beta\frac{d}{dy}\left(\frac{du}{dy}\right)^3 - \frac{1}{K}\left[1 + 2\beta\left(\frac{du}{dy}\right)^2\right]u - Mu = C, \quad (5.36)$$

with boundary conditions

$$u(-1) = 0 \qquad u(1) = 0. \quad (5.37)$$

The effects of magnetic, porosity, pressure gradient and third grade parameters for fully developed plane Poiseuille flow in the presence of applied pressure gradient are shown in Figs. 7 to 10.

5.4 Generalized plane Couette Flow Problem

Here flow is induced due to applied pressure gradient and sudden motion of upper plate. Thus the equation is

$$\frac{d^2u}{dy^2} + 2\beta\frac{d}{dy}\left(\frac{du}{dy}\right)^3 - \frac{1}{K}\left[1 + 2\beta\left(\frac{du}{dy}\right)^2\right]u - Mu = C, \quad (5.38)$$

with boundary conditions

$$u(0) = 0 \qquad u(2) = 1. \quad (5.39)$$

Figs. 11 to 14 illustrate the generalized plane Couette flow due to applied pressure gradient and sudden motion of upper plate.

6 Conclusions

In this article, four fundamental flow problems are tested numerically through the employed Scheme. Highly nonlinear problems are solved by this procedure. Through comparative study of the presented results, the following observations are worth-mentioning.

1. The velocity is decreasing function of magnetic parameter M in plane Couette flow.

2. Magnitude of velocities in Plug Poiseuille and generalized Couette flows is qualitatively similar to that of Couette flow.

3. Effects of permeability parameter (K) on the velocity in all the considered flows are opposite to that of the magnetic parameter.

4. The magnitude of velocity in third grade fluid is much when compared with the viscous fluid. This observation holds for all the considered flow cases.

5. Magnitude of velocity in presence of adverse pressure gradient is decreased when Poiseuille and generalized Couette flows are studied.

Acknowledgments

The authors acknowledge financial support from the Imam Khomeini International University project IKIU-11552. The authors would like to thank anonymous referees for valuable suggestions.

References

[1] M. Nazar, C, Fetecau, D. Vieru, C. Fetecau, *New exact solutions corresponding to the second problem of Stokes for second grade fluids*, Nonlinear Analysis: Real World Applications 1 (2010) 584-591.

[2] M. Keimanesh, M. M. Rashidi, A. J. Chamkha, R. Jafari, *Study of a third grade non-Newtonian fluid flow between two parallel plates using the multi-step differential transform method*, Computers and Mathematics with Application 62 (2011) 2871-2891.

[3] S. Abbasbandy, T. Hayat, R. Ellahi and S. Asghar, *Numerical results of flow in a third grade fluid between two porous walls*, Zeitschrift Fur Naturforschung A 64 (2009) 59-64.

[4] S. Abbasbandy, T. Hayat, F. M. Mahomed and R. Ellahi, *On comparison of exact and series solutions for thin film flow of a third grade fluid*, International Journal of Numerical Method in Fluids 61 (2009) 987-994.

[5] W. C. Tan, T. Masuoka, *Stokes' first problem for a second grade fluid in a porous half space with heated boundary*, Int. J. Non-Linear Mech. 40 (2005) 512-522.

[6] W. C. Tan and T. Masuoka, *Stokes' first problem for an Oldroyd-B fluid in a porous half space*, Phys. Fluids 17 (2005) 23101-23107.

[7] G. Liu,Y. Gu, *An introduction to meshfree methods and their programing*, Springer. 2005.

[8] T. Belytschko,Y. Y. Lu, L. Gu, *Element-free Galerkin methods*, International Journal for Numerical Methods in Engineering 37 (1994) 229-256.

[9] T. Belytschko, Y. Y. Lu, L. Gu, *Element free Galerk in methods for static and dynamic fracture*, International Journal of Solids and Structures 32 (1995) 2547-2570.

[10] E. Kansa, *Multiquadrics – A scattered data approximation scheme with applications to computational fluid-dynamics – I: Surface approximations and partial derivative estimates*, Computers & Mathematics with Applications 19 (1990) 127-145.

[11] M. Dehghan, A. Shokri, *A numerical method for solution of the two dimensional sine-Gordon equation using the radial basis functions*, Mathematics and Computers inSimulation 79 (2008) 700-715.

[12] L. Ling, R. Opfer, R. Schaback, *Results on meshless collocation techniques*, Engineering Analysis with Boundary Elements 30(4) (2006) 247-253.

[13] L. Ling, R. Schaback, *Stable and convergent unsymmetric meshless collocation methods*, SIAM Journal of Numerical Analysis 46 (2008) 1097-1115.

[14] N. Libre, A. Emdadi, E. Kansa, M. Shekarchi, M. Rahimian, *A fast adaptive wavelet scheme in RBF collocation for nearly singular potential PDEs*, Computer Modeling in Engineering and Sciences 38 (2008) 263-284.

[15] N. Libre, A. Emdadi, E. Kansa, M. Shekarchi, M. Rahimian, *A multi resolution prewavelet-based adaptive refinement scheme for RBF approximations of nearly singular problems*, Engineering A nalysis with Boundary Elements 33 (2009) 901-914.

[16] S. Atluri, T. Zhu, *A new meshless local Petrov-Galerkin (MLPG) approach in computational mechanics*, Computational Mechanics 22 (1998) 117-127.

[17] S. Atluri, T. Zhu, *A new meshless local Petrov–Galerkin (MLPG) approach to nonlinear problems in computer modeling and simulation*, Computer Modeling & Simulation in Engineering 3 (1998) 187-196.

[18] S. Atluri, T. Zhu, *New concepts in meshless methods*, International Journal of Numerical Methods in Engineering 13 (2000) 537-56.

[19] S. Atluri, T. Zhu, *The meshless local Petrov-Galerkin (MLPG) approach for solving problems in elasto-statics*, Computational Mechanics 25 (2000) 169-179.

[20] M. Dehghan, D. Mirzaei, *The meshless local Petrov–Galerkin (MLPG) method for the generalized two-dimensional non-linear Schrödinger equation*, Eng. Anal. Bound. Elem. 32 (2008) 747-756.

[21] M. Dehghan, D. Mirzaei, *Meshless local Petrov-Galerkin (MLPG) method for the unsteady magnetohydrodynamic (MHD) flow through pipe with arbitrary wall conductivity*, Appl. Numer. Math. 59 (2009) 1043-1058.

[22] Y. Gu, G. Liu, *A meshless local Petrov-Galerkin (MLPG) method for free and forced vibration analyses for solids*, Computational Mechanics 27 (2001) 188-198.

[23] A. Shirzadi, L. Ling, S. Abbasbandy, *Meshlesss imulations of the two-dimensional fractional-time convection-diffusion-reaction equations*, Engineering Analysis with Boundary Elements 36 (2012) 1522-1527.

[24] B. Nayroles, G. Touzot, P. Villon, *Generalizing the finite element method: diffuse approximation and diffuse elements*, Comput. Mech. 10 (1992) 307-318.

[25] A. G. Bratsos, *An improved numerical scheme for the sine-Gordon equation in 2+1 dimensions*, Int. J. Numer. Meth. Eng. 75 (2008) 787-799.

[26] P. W. *Clear, Modeling conned multi-material heat and mass flows using SPH*, Appl. Math. Model. 22 (1998) 981-993.

[27] W. K. Liu, S. Jun, Y. F. Zhang, *Reproducing kernel particle methods*, Int. J. Numer. Meth. Eng. 20 (1995) 1081-1106.

[28] Y. X. Mukherjee, S. Mukherjee, *Boundary node method for potential problems*, Int. J. Numer. Meth. Eng. 40 (1997) 797-815.

[29] J. M. Melenk, I. Babuska, *The partition of unity finite element method: Basic theory and applications*, Comput. Meth. Appl. Mech. Eng. 139 (1996) 289-314.

[30] S. De, K. J. Bathe, *The method of finite spheres*, Comput. Mech. 25 (2000) 329-345.

[31] Y. Gu, G. A. Liu, *boundary point interpolation method for stress analysis of solids*, Computational Mechanics 28 (2002) 47-54.

[32] Y. T. Gu, G.R. Liu, *A boundary radial point interpolation method (BRPIM) for 2-D structural analyses*, Struct. Eng. Mech. 15 (2003) 535-550.

[33] G. R. Liu, L. Yan, J. G. Wang, Y. T. Gu, *Point interpolation method based on local residual formulation using radial basis functions*, Struct. Eng. Mech. 14 (2002) 713-732.

[34] G. R. Liu, Y. T. Gu, *A local radial point interpolation method (LR-PIM) for free vibration analyses of 2-D solids*, J. Sound Vib. 246 (2001) 29-46.

[35] M. Dehghan, A. Ghesmati, *Numerical simulation of two-dimensional sine- gordon solitons via a local weak meshless technique based on the radial point interpolation method (RPIM)*, Computer Physics Communications, 181 (2010) 772-786.

[36] E. Shivanian, *Analysis of meshless local radial point interpolation (MLRPI) on a nonlinear partial integro-differential equation arising in population dynamics*, Eng. Anal. Boundary Elem. 37 (2013) 1693-1702.

[37] J. G. Wang, G. R. Liu, *A point interpolation meshless method based on radial basis functions*, Int. J. Numer. Meth. Eng. 54 (2002) 1623-1648.

[38] J. G. Wang, G. R. Liu, *On the optimal shape parameters of radial basis functions used for 2-D meshless methods*, Comput. Meth. Appl. Math. 191 (2002) 2611- 2630.

[39] C. Franke, R. Schaback, *Solving partial differential equations by collocation using radial basis functions*, Applied Mathematics and Computation 93 (1997) 73-82.

[40] M. Sharan, E. J. Kansa, S. Gupta, *Application of the multiquadric method for numerical solution of elliptic partial differential equations*, Appl. Math. Comput. 84 (1997) 275-302.

[41] M. J. D. Powell, *Theory of radial basis function approximation in 1990, in: F.W. Light(Ed.)*, Adv. Numer. Anal. 4 (1992) 303-322.

[42] H. Wendland, *Error estimates for interpolation by compactly supported radial basis functions of minimal degree*, Journal of Approximation Theory 93 (1998) 258-396.

Saeid Abbasbandy has got PhD degree from Kharazmi University in 1996 and now he is the full professor in Imam Khomeini International University, Ghazvin, Iran. He has published more than 200 papers in international journals and conferences. Now, he is working on numerical analysis and fuzzy numerical analysis.

Dr. Elyas Shivanian was born in Zanjan province, Iran in August 26, 1982. He started his master course in applied mathematics in 2005 at Amirkabir University of Technology and has finished MSc. thesis in the field of fuzzy linear programming in 2007. After his Ph.D. in the field of prediction of multiplicity of solutions of boundary value problems, at Imam Khomeini International University in 2012, he became an Assistant Professor at the same university. His research interests are analytical and numerical solutions of ODEs, PDEs and IEs. He has several papers on these subjects. He also has published some papers in other fields, for more information see http://scholar.google.com/citations?user=MFncks8AAAAJ&hl=en